Unexpected Selective Gas Adsorption on a 'Non-Porous' Metal Organic Framework

Stuart Beveridge [1,2], Craig A. McAnally [1,2], Gary S. Nichol [3], Alan R. Kennedy [2], Edmund J. Cussen [2,4,*] and Ashleigh J. Fletcher [1,*]

[1] Department of Chemical and Process Engineering, University of Strathclyde, James Weir Building, Glasgow G1 1XJ, UK; beveridge.stuart@outlook.com (S.B.); craig.mcanally@googlemail.com (C.A.M.)

[2] Department of Pure and Applied Chemistry, University of Strathclyde, Thomas Graham Building, Glasgow G1 1XL, UK; a.r.kennedy@strath.ac.uk

[3] School of Chemistry, University of Edinburgh, Joseph Black Building, Edinburgh EH9 3FJ, UK; g.s.nichol@ed.ac.uk

[4] Department of Materials Science and Engineering, University of Sheffield, Sir Robert Hadfield Building, Mappin Street, Sheffield S1 3JD, UK

* Correspondence: e.j.cussen@sheffield.ac.uk (E.J.C.); ashleigh.fletcher@strath.ac.uk (A.J.F.)

Abstract: A metal organic framework $Cu(tpt)BF_4 \cdot \frac{3}{4}H_2O$ was synthesized as a potential carbon capture material, with the aim being to exploit the Lewis base interaction of the incorporated ligand functionalities with acidic gas. The material displays high thermal stability but an exceptionally low surface area; however, this contrasts starkly with its ability to capture carbon dioxide, demonstrating significant activated diffusion within the framework. The full characterization of the material shows a robust structure, where the CO_2 sorption is 120% greater than current industrial methods using liquid amine solutions; the thermal energy required for sorbent regeneration is reduced by 65%, indicating the true industrial potential of the synthesized material.

1. Introduction

Anthropogenic activities, including increased industrialization, have resulted in increased greenhouse gas emissions that have resulted in increased worldwide temperatures, which are linked to global warming; this explains recent efforts to ameliorate such discharges in line with international legislative protocols [1,2]. Strategies include carbon capture and sequestration, both of which allow for the continued use of fossil fuels to supply the world's increasing energy demand, while reducing greenhouse gas emissions. Post-combustive capture is of significant interest, as it is easily retrofitted to existing facilities, and can be used with either bulk liquid amines or the emerging range of porous solid materials. Amine scrubbing carries a high (up to 35%) energy penalty [3] where solvent recovery accounts for ~ 80% of energy demand [4], while the chemicals used are extremely corrosive, requiring additives and inhibitors to control corrosion and oxidation [5]. Such energy demands can be reduced by utilizing solid capture materials, which negate the need to pump large liquid volumes within the system and involve physisorbed processes that require lower regeneration energies than their chemisorbed counterparts, such as liquid amines.

Doping solid sorbents with amine functionalities allows for the high affinity of Lewis base nitrogen-containing groups for acidic gases, such as carbon dioxide, to be exploited, while also acting to immobilize such functionalities in a benign host with increased accessibility for adsorptive species. Solid sorbents include zeolites, which demonstrate molecular sieving but generally suffer

low CO_2 capacities, poor CO_2/N_2 selectivities and hygroscopic tendencies; their regeneration is less energy intensive than bulk amines (<20% [6]) but they undergo significant structural degradation on cycling. Activated carbons offer a family of cheap, readily available sorbents with large surface areas, increased hydrophobicity, and reductions in cyclical decomposition and energies of regeneration; however, sample variability is a significant issue and uptake can be very low under sub-atmospheric pressures, where the interactions are purely physical in nature, leading to poor affinity with CO_2, reducing capacities and increasing charging periods. Metal organic frameworks (MOFs) are a family of structured coordination complexes composed of repeating units of metal connectors and organic ligand linkers. A subset of these materials can be evacuated of their guest species to leave porous solids capable of adsorption behaviors, and several exhibit large surface areas, but thermal stability, especially under a vacuum, can be an issue for many of these materials. The organic ligands present within MOFs allow useful functionalities to be incorporated into the structure, such as amines, fluoroalkanes and open metal centers [7], which may be attractive to CO_2. While some researchers [8] have focused on forming composites to enhance the porous character of MOFs, many already possess significant void space; however, the initial characterization of such materials may infer a lack of porosity and preclude such materials from further study. Here, we focus on the gas sorption properties of a material classified as non-porous by crystallographic and textural adsorption measurements.

2. Results and Discussion

In this study, $Cu(tpt)BF_4 \cdot 3/4H_2O$ was synthesized using an excess of $Cu(BF_4)_2$, producing a yield of 68% with respect to the ligand tpt (2,4,6-Tri(4-pyridyl)-1,3,5-triazine). Following solvent exchange, to aid ion exchange and to maximize retention of porous character, single crystal X-ray diffraction was performed; the extended structure of the crystal creates planes of arranged, repeating tpt units, held together by Cu^{1+} atoms, with each plane of tpt perpendicular to the one above and below, creating a 3D skeletal crystal network with pores (Figure 1) similar to $[Cu_3(tpt)_4](BF_4)_3(tpt)_{2/3} \cdot 5H_2O$, previously reported by Dybtsev et al. [9]; in contrast, the latter structure consists of a copper center surrounded by four tpt ligands in a tetrahedral arrangement but could not be obtained solvothermally. The sample phase purity of $Cu(tpt)BF_4 \cdot 3/4H_2O$ was confirmed using powder X-ray diffraction.
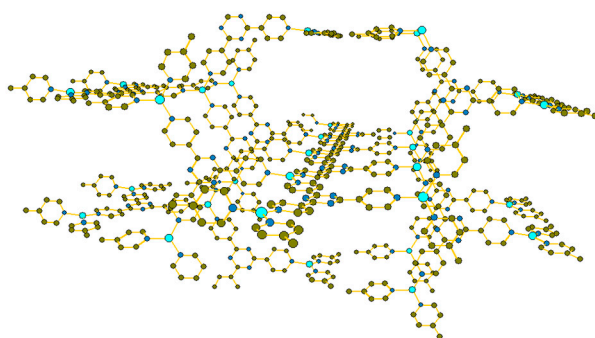

Figure 1. Depth perspective of $Cu(tpt)BF_4 \cdot \frac{3}{4}H_2O$ skeletal framework. Hydrogen atoms omitted for clarity.

The determined structure may be expected to create a very open and porous skeletal framework; however, the crystal structure consists of four interpenetrating layers arranged as parallel crystal sheets (Figure 2), resulting in a high degree of π interactions from the aromatic tpt units, and hence the increased thermal stability of the material (see Supplementary Materials). The interpenetrating layers are π-stacked at a distance of 3.2 Å, and arranged in order to maximize the attractive forces by alternating out-of-phase layers (Figure 3b,c), creating 'off-set' π-stacking interactions both above and below the plane, which have previously been documented as highly preferential within metal complexes with aromatic, nitrogen-containing ligands [10].
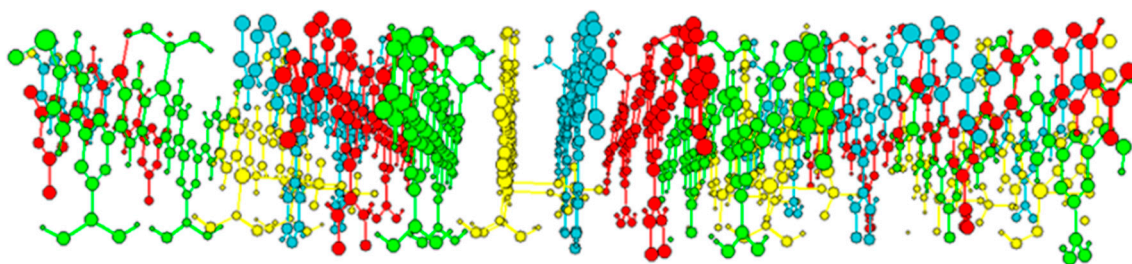
Figure 2. Four-layer interpenetration arrangement of $Cu(tpt)(BF_4) \cdot \frac{3}{4}H_2O$ crystal structure. Guest species omitted for clarity.
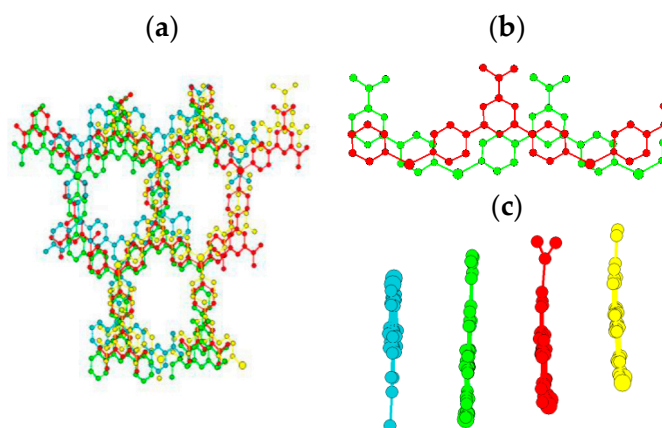
(**a**)   (**b**)

(**c**)

Figure 3. (**a**) Interpenetrated network with pores along a-axis; (**b**) parallel displaced π-stacking between interpenetrating layers, with π-stacking distances of 3.2 Å (**c**) side view of displacement. Guest species and hydrogen atoms omitted for clarity.

In contrast, Dybtsev's material [9] contains two interpenetrating layers with face-to-face π-π interactions separated by 3.5 Å, similar to the stacking observed by Wu et al. for a rhenium metalloprism containing tpt [11], while several other groups report spacings of 3.4 Å–3.6 Å [12–14]. The decrease in π-stacking distance for the material reported here is a result of the 'off-set' π-stacking arrangement, strengthening interactions, and currently represents the closest stacking observed for a tpt-containing framework. A disadvantage of such interpenetration is the closure or blockage of pore channels created by the original structure, as seen from Figure 2; when transforming the material from a 3D porous material to a 1D porous material along the a-axis (Figure 3a), with dimensions of 9 × 13 Å hosting water and tetrafluoroborate molecules, with one $(BF_4)^-$ per copper, there is a reduction in the Cu^{2+} reactant during the reaction to Cu^{1+} within the product formed (as observed during synthesis via color change, and confirmed via bond valence summation; such behavior has been observed in previous studies [15–18]). In contrast to the close tpt packing, the 2.67 Å Cu^{1+}-$(BF_4)^-$ distance is much longer than typical Cu-F bond lengths (1.90–1.93 Å), suggesting that no formal bond exists, but merely an attractive stabilizing interaction between Cu^{1+} and $(BF_4)^-$, indicating anion exchange to a smaller anion, e.g., Cl^-, and hence that open metal sites (OMS) may be possible. Consequently, the $(BF_4)^-$ acts as a templating and charge-balancing species that orients the organic ligand. Where the individual crystal planes interface perpendicularly, the first aromatic unit rotates around the σ-bonds connecting the pyridine to either the Cu^{1+} or the triazine ring; the orientation of this section of tpt is directed so that the edge of the ring points towards the closest anion, creating a stabilizing interaction similar to face-to-edge π-stacking. The copper ligands are structured in a trigonal planar arrangement, which is known [19], but uncommon for Cu^{1+}, which, as a d^{10} species, is traditionally tetrahedral in shape, preferring either two or four coordinates, with the three-coordinate trigonal planar arrangement giving a higher energy conformation [20].

Surface area analysis, using N_2 adsorption at 77 K, shows the material to be non-porous with a small BET surface area of <7 m^2 g^{-1}, as determined by Brunauer-Emmett-Teller (BET) theory [21] using data acquired from an ASAP2420 (Micromeritics, UK); however, gravimetric CO_2 adsorption analysis at 273 K (Intelligent Gravimetric Analyzer (IGA003), Hiden Isochema, UK) showed an uptake of 1.8 mmol g^{-1} at 10 bar (Figure 4), which equates to 7.6 wt%, with a sharp initial increase up to 1 bar, attributed to attractive surface interactions between the material and CO_2 once saturated pore filling occurs. This discrepancy between adsorption uptakes for the two gases is ascribed to activated diffusion effects at the low temperatures used in N_2 adsorption analysis, which is consistent with the pore restrictions invoked by interpenetration of the framework. Marked hysteresis is observed at pressures below 5 bar; the Type I isotherm obtained indicates that this is not the result of mesoporous character, but rather demonstrates an increased attraction between the material and adsorbed CO_2 on desorption, with significant retention observed below 500 mbar. This suggests an interaction strength greater than typical physisorption interactions, the system was heated to 403 K under vacuum to regenerate the material with a relaxation back to zero mass observed above 373 K. The activated diffusion observed for N_2 adsorption causes slow adsorption kinetics for CO_2 even at 273 K; additional activation (433 K under vacuum for 12 h, which equates to 737 K at atmospheric conditions by ASTM D2892-13 [22]) showed little supplementary mass loss, but resulted in an enhanced CO_2 uptake at low pressure, ascribed to the degassing of additional porosity, hence the attractive sites within the material. The overall uptake remains unchanged; however, the increased uptakes at lower pressures indicate improved performance within industrially relevant regimes, which may be further increased by the supercritical solvent exchange of the material prior to adsorption. It is notable that a Langmuir analysis gives a surface area >200 m^2 g^{-1} for this material. The uptake observed compares favorably with established methods of carbon capture; monoethanolamine (MEA) can theoretically capture 0.5 mol CO_2/mol MEA, but is practically limited to 0.44 mol CO_2/mol MEA due to degradation [23], while the material produced here shows 0.8 mol CO_2/mol Cu(tpt)$BF_4 \cdot \frac{3}{4} H_2O$, approaching the expected uptake of one CO_2 molecule per tpt ligand. Combined with the high regenerative energy penalty for MEA, where 403 K is routinely required for complete desorption, i.e., 165 kJ mol^{-1} of CO_2 regenerated [4], our material requires 58 kJ mol^{-1} (based on heating to 373 K and a determined specific heat capacity of 0.9 kJ kg^{-1} K^{-1}, see Supplementary Materials), representing a significant decrease in regenerative thermal energy.
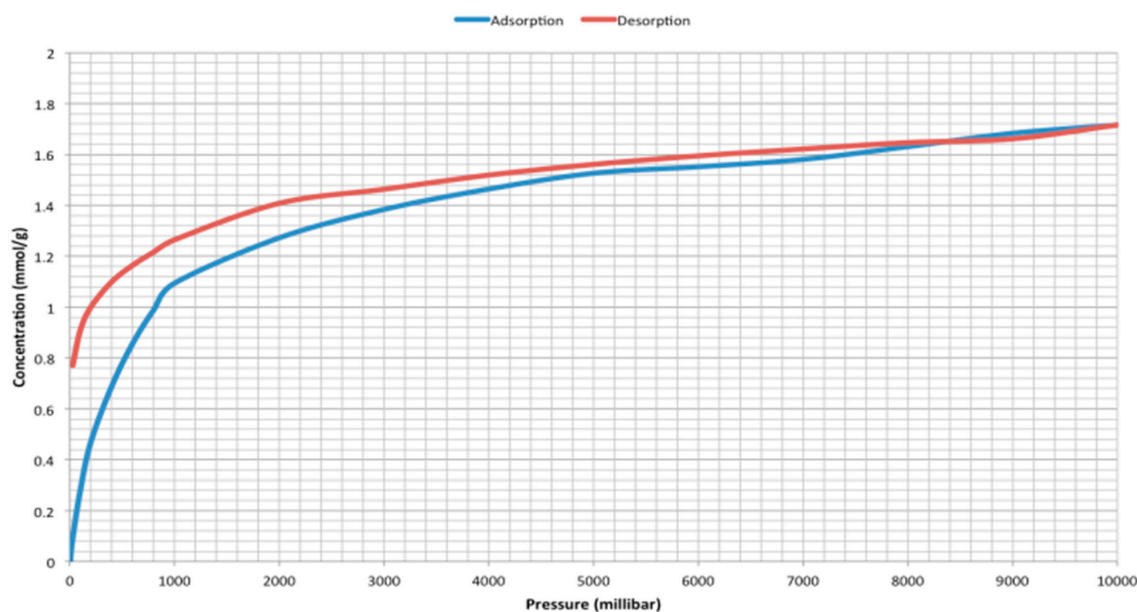

Figure 4. CO_2 sorption isotherms on Cu(tpt)$(BF_4) \cdot \frac{3}{4} H_2O$ at 273 K.

The probe gases used in this study have similar kinetic diameters: carbon dioxide 3.3 Å and nitrogen 3.6 Å [24], and the pore diameter of 9 Å × 13 Å should allow both molecules to diffuse into the framework, however, the electron cloud density associated with the molecular units comprising the framework, as well as the thermal expansion and vibrational movement of the atoms themselves, result in an effective decrease to a non-uniform pore diameter that is constantly altered in terms of shape and size. In addition to the electron cloud movement experienced by the adsorptive gas, the system exhibits activated diffusion, which is marked at the low temperatures used for N_2 adsorption. The diffusion of gases in solids generally obeys an Arrhenius-type relationship, whereby an increase in temperature increases the rate of diffusion as determined by Fick's first law of diffusion [25], and arises from the different thermal states of the adsorptive gases; CO_2 adsorption was measured at 273 K, and N_2 at 77 K, equating to reduced temperatures of 0.90 and 0.61, respectively. Thus, CO_2 is in a higher thermal state than N_2, thus the surrounding electron cloud will be of a higher energy, and hence it can be more easily manipulated to fit the constricted pore.

A new metal organic framework is reported, which appears non-porous by classical characterization methods but shows high affinity for CO_2. The material demonstrates exceptional thermal stability; the central Cu^{1+} atoms are in a high energy, unfavored coordination state of three ligands in a trigonal planar structure; however, π-stacking between the interpenetrating layers strengthens the material. The microporous nature of the material causes activated diffusion, as determined by comparison of N_2 adsorption at 77 K and CO_2 adsorption at 273 K, as shown by the isotherms and surface areas obtained, resulting in 7.6 wt% of CO_2 adsorbed. The material demonstrates advantages over traditional amine scrubbing systems, with the potential for utilization in a combined pressure and temperature swing adsorption process.

3. Methodology

3.1. Synthesis of 2,4,6-tri(4-pyridyl)-1,3,5-triazine (tpt)

In total, 8.97 g (86.2 mmol) 4-cyanopyridine (98%, Acros Organics, UK) was ground to a fine powder; separately, 1 g (3.8 mmol) 18-crown-6 (Fluorochem, UK; added to increase the ability of the hydroxyl group to perform a nucleophilic addition reaction on the nitrile group [26]) and 0.23 g (4.0 mmol) potassium hydroxide (Sigma Alcrich, UK) were added to 15 mL methanol and left to evaporate, resulting in the formation of an oil, which was placed within a 23 mL Teflon autoclave liner, along with the cyanopyridine, sealed within a stainless steel autoclave, and placed inside an oven (UFP400, Memmert, UK), then heated to 200 °C for 7 h, before cooling for 30 h at 0.1°C min^{-1}. The product was purified (see Supplementary Materials) by washing with 50 mL 50/50 H_2O/EtOH (in-house distilled/Sigma Aldrich) in a vacuum filtration set up, air dried, then boiled in 50 mL of 50/50 H_2O/EtOH for 30 min, vacuum filtered and dried in air.

3.2. Solvothermal Synthesis of Cu(tpt)(BF4)·$\frac{3}{4}$H$_2$O

0.1 g (0.32 mmol) of 2,4,6-tri(4-pyridyl)-1,3,5-triazine (tpt) was added to a 23 mL Teflon autoclave liner, to which 0.221 g (0.64 mmol) Cu(BF$_4$)$_2$·6H$_2$O (Sigma Aldrich, UK) was added, along with 10 mL methanol (Sigma Aldrich, UK) and this was then stirred for 15 min before sealing it within a stainless steel autoclave (Anton Parr, UK) heated to 160 °C and holding it for 48 h, before cooling at 10 °C h^{-1} to room temperature (yield 67.8%). Once cooled, the mother liquor was extracted, and the solid product was repeatedly washed with clean methanol to remove impurities before cyclonic separation. The resulting sample was solvent exchanged with fresh methanol daily for 3 d and, finally, dried in air.

Full single crystal X-ray diffraction (SCXRD) refinement and adsorption data are available within the Supplementary Materials.

Supplementary Materials: The following are available online at http://www.mdpi.com/2073-4352/10/6/548/s1, Table S1: Crystal Data and Structure Refinement for [Cu(tpt)][BF4]·$\frac{3}{4}$H$_2$O, Figure S1: IR Spectra of unpurified tpt (blue), and purified tpt (red), Figure S2: Comparison of PXRD across three produced samples of the produced

MOF, Figure S3: Comparison of: (top) Simulated powder X-ray diffraction pattern based upon single crystal analysis; (bottom) Experimental powder X-ray diffraction patterns for three different samples, Figure S4: TGA and DSC of Cu(tpt)BF4·$\frac{3}{4}$H$_2$O, Figure S5: Calculated heat capacity across the full DSC range of 40°C–290°C, Figure S6: Adsorption isotherm for N$_2$ on Cu(tpt)BF4·$\frac{3}{4}$H$_2$O at 77 K, Figure S7: BET plot from Rouquerol transform data for adsorption of N$_2$ on Cu(tpt)BF$_4$·$\frac{3}{4}$H$_2$O at 77 K, Figure S8: Selected area (0.04 ≤ P/Po ≤ 0.11) BET fit for adsorption of N$_2$ on Cu(tpt)BF4·$\frac{3}{4}$H$_2$O at 77 K, Figure S9: Adsorption isotherm for CO$_2$ on Cu(tpt)BF4·$\frac{3}{4}$H$_2$O at 273 K modeled to Langmuir adsorption model.

References

1. Intergovernmental Panel on Climate Change. *Intergovernmental Panel on Climate Change (IPCC) Fifth Assessment Report: Climate Change 2014*; Intergovernmental Panel on Climate Change: Geneva, Switzerland, 2014.

2. United Nations. *Kyoto Protocol to the United Nations Framework Conventions on Climate Change*; United Nations: New York, NY, USA, 1998.

3. Global CCS Institute. *CO$_2$ Capture Technologies—Post Combustion Capture (PCC)*; Global CCS Institute: Melbourne, Australia, 2012.

4. Pennline, H.W.; Resnik, K.P.; Yeh, J.T. Study of CO$_2$ Absorption and Desorption in a Packed Column. *Energy Fuels* **2001**, *15*, 274–278.

5. Booras, G.S.; Smelser, S.C. An engineering and economic evaluation of CO$_2$ removal from fossil-fuel-fired power plants. *Energy Environ. Sci.* **1991**, *16*, 1295–1305. [CrossRef]

6. Zhang, J.; Webley, P.A.; Xiao, P. Effect of process parameters on power requirements of vacuum swing adsorption technology for CO$_2$ capture from flue gas. *Energy Convers. Manag.* **2008**, *49*, 346–356. [CrossRef]

7. Sumida, K.; Rogow, D.; Mason, J. Carbon dioxide capture in metal-organic frameworks. *Chem. Rev.* **2011**, *112*, 724–781. [CrossRef] [PubMed]

8. He, Y.; Shang, J.; Zhao, Q.; Gu, Q.; Xie, K.; Li, G.; Singh, R.; Xiao, P.; Webley, P.A. A comparative study on conversion of porous and non-porous metal–organic frameworks (MOFs) into carbon-based composites for carbon dioxide capture. *Polyhedron* **2016**, *120*, 30–35. [CrossRef]

9. Dybtsev, D.N.; Chun, H.; Kim, K. Three-dimensional metal–organic framework with (3,4)-connected net, synthesized from an ionic liquid medium. *Chem. Commun.* **2004**, *14*, 1594–1595. [CrossRef] [PubMed]

10. Janiak, C. A critical account on π-π stacking in metal complexes with aromatic nitrogen-containing ligands. *J. Chem. Soc. Dalton Trans.* **2000**, *21*, 3885–3896. [CrossRef]

11. Wu, J.-Y.; Chang, C.-H.; Thanasekaran, P.; Tsai, C.-C.; Tseng, T.-W.; Lee, G.-H.; Peng, S.-M.; Lu, K.-L. Unusual face-to-face pi-pi stacking interactions within an indigo-pillared M$_3$ (tpt)-based triangular metalloprism. *Dalton Trans.* **2008**, *135*, 6110–6112. [CrossRef] [PubMed]

12. Abrahams, B.F.; Batten, S.R.; Hamit, H.; Hoskins, B.F.; Robson, R. A wellsian 'three-dimensional' racemate: Eight interpenetrating, enantiomorphic (10,3)-a nets, four right- and four left-handed. *Chem. Commun.* **1996**, *11*, 1313. [CrossRef]

13. Abrahams, B.F.; Batten, S.R.; Hamit, H.; Hoskins, B.F.; Robson, R. A Cubic (3, 4)-Connected Net with Large Cavities in Solvated [Cu$_3$(tpt)$_4$](ClO$_4$)$_3$ (tpt = 2,4,6-Tri (4-pyridyl)-1,3,5-triazine). *Angew. Chem. Int. Ed. Engl.* **1996**, *35*, 1690–1692. [CrossRef]

14. Batten, S.R.; Hoskins, B.F.; Robson, R. Two Interpenetrating 3D Networks Which Generate Spacious Sealed-Off Compartments Enclosing of the Order of 20 Solvent Molceules in the Structures of Zn (CN)(NO$_3$)(tpt) ^{2}/$_3$. cntdot. solv (tpt = 2,4,6-tri (4-pyridyl)-1,3,5-triazine, solv = apprx. ^{3}/$_4$C$_2$H$_2$Cl$_4$. cntdot. ^{3}/$_4$CH$_3$OH or. apprx. ^{3}/$_2$CHCl$_3$. cntdot. 1/3CH$_3$OH). *J. Am. Chem. Soc.* **1995**, *117*, 5385–5386.

15. Singh, S. Cu (I)/Ag (I)-3-(2-Pyridyl)-5, 6-diphenyl-1, 2, 4-triazine-p, p'-disulfonate Based Coordination Polymers: Synthesis, Structures and Photoluminescent Properties. *ChemistrySelect* **2018**, *3*, 6786–6790. [CrossRef]

16. Jin, C.-M.; Zhu, Z.; Yao, M.-X.; Meng, X.-G. In situ reduction from CuX_2 (X = Br, Cl) to Cu (I) halide clusters based on ligand bis (2-methylimidazo-1-yl) methane. *CrystEngComm* **2010**, *12*, 358–361. [CrossRef]

17. Jana, S.; Bhowmik, P.; Chattopadhyay, S. Unique in situ reduction of copper (ii) forming an interesting photoluminescent stair-polymer of copper (i) with a $Cu_2 S_2$ core. *Dalton Trans.* **2012**, *41*, 10145–10149. [CrossRef] [PubMed]

18. Banthia, S.; Samanta, A. In situ reduction of copper (II) forming an unusually air stable linear complex of copper (I) with a fluorescent tag. *Inorg. Chem.* **2004**, *43*, 6890–6892. [CrossRef] [PubMed]

19. Greenwood, N.N.; Earnshaw, A. Copper, Silver and Gold Complexes. In *Chemistry of the Elements*; Butterworth Heinemann: Waltham, MA, USA, 1998.

20. Pavelka, M.; Burda, J.V. Theoretical description of copper Cu(I)/Cu(II) complexes in mixed ammine-aqua environment. DFT and ab initio quantum chemical study. *Chem. Phys.* **2005**, *312*, 193–204. [CrossRef]

21. Brunauer, S.; Emmett, P.H.; Teller, E. Adsorption of gases in multimolecular layers. *J. Am. Chem. Soc.* **1938**, *60*, 309–319. [CrossRef]

22. American Society for Testing and Materials. *ASTM D2892-13 Standard Test Method for Distillation of Crude Petroleum*; American Society for Testing and Materials: West Conshohocken, PA, USA, 2013.

23. Mazari, S.A.; Ali, B.S.; Jan, B.M.; Saeed, I.M.; Nizamuddin, S. An overview of solvent management and emissions of amine-based CO_2 capture technology. *Int. J. Greenh. Gas Control* **2015**, *34*, 129–140. [CrossRef]

24. Webster, C.E.; Drago, R.S.; Zerner, M.C. Molecular dimensions for adsorptives. *J. Am. Chem. Soc.* **1998**, *120*, 5509–5516. [CrossRef]

25. Fick, A. Ueber diffusion. *Annalen der Physik* **1855**, *170*, 59–86. [CrossRef]

26. Steed, J.W.; Atwood, J.L. *Supramolecular Chemistry*; John Wiley & Sons: Hoboken, NJ, USA, 2013.